

Original Article

Impact of fluoride on ameloblasts and MAPKs and caspase-12 activity in the tooth germ of rat offspring

Lin Zhao^{1,2}, Jia-Li Su^{1,3}, Ning Dong¹, Jue-Dan Li¹, Yan Liu¹, Peng Wang¹, Jian-Ping Ruan¹

¹Clinical Research Center of Shaanxi Province for Dental and Maxillofacial Diseases, Department of Preventive Dentistry, Stomatology Hospital, Xi'an Jiaotong University, No. 98 Xiwu Road, Xi'an 710004, Shaanxi Province, China; ²Ningxia Medical University, No. 1160 Shengli Street, Yinchuan 750021, Ningxia Hui Autonomous Region, China; ³Yinchuan Stomatology Hospital, No. 85 Jiefang East Street, Yinchuan 750004, Ningxia Hui Autonomous Region, China

Received November 2, 2016; Accepted February 4, 2017; Epub March 1, 2017; Published March 15, 2017

Abstract: Fluoride has been proved to transmit from mother to child; however, the impact of fluoride on ameloblasts has not been fully demonstrated in rat offspring. This study aimed to evaluate the effect of fluoride on ameloblasts in the offspring rat tooth germ. Male and female rats were given 50 (low-fluoride group) or 100 mg/L fluoride-containing water (high-fluoride group) for successive 6 weeks, while those given fluoride-free water served as controls. The offspring rats were sacrificed 3 days after birth, and mandibular tooth germ was collected for the subsequent experiments. Obvious yellow-brown or white streaks were observed in the incisor of rats given fluoride-containing water. Optical microscopy showed vacuolar changes in ameloblasts in the high-fluoride group, while no apparent changes were seen in the low-fluoride group or controls. Transmission electron microscopy displayed scattered vacuoles and enlargement of rough endoplasmic reticulum in the low-fluoride group. TUNEL assay showed yellow-brown granules in ameloblasts in the high-fluoride group, while no granules found in controls or the low-fluoride group. Immunohistochemical staining and Western blotting detected positive p-ERK, p-JNK and p-p38 expression on ameloblasts in controls, and p-ERK and p-JNK expression reduced but p-p38 expression increased with fluoride concentration ($P < 0.05$), while caspase-3, caspase-8, caspase-9 and caspase-12 expression reduced with fluoride concentration ($P < 0.05$). Our findings demonstrate that high-concentration fluoride causes morphological and ultrastructural changes and apoptosis in the tooth germ ameloblasts of rat offspring. In addition, MAPK signaling is linked to dental fluorosis, and caspase-12 may be involved in fluoride-induced ameloblast apoptosis.

Keywords: Fluoride, ameloblast, apoptosis, dental fluorosis, MAPK, caspase-12, rat offspring

Introduction

Dental fluorosis, caused by ingestion of excessive fluoride during tooth development, is a permanent hypo-mineralization of tooth enamel, which is characterized by emergence of yellow tooth, white streaks, browning of spots and mottling of enamel [1, 2]. As a global disease, the prevalence of dental fluorosis varies in countries [3]. In China, the prevalence of this endemic disease also varies in regions, ranging from 5% to over 95% [4].

The mitogen activated protein kinase (MAPK) family, which includes three subfamilies of extracellular-regulated protein kinase (ERK), c-Jun N-terminal kinase or stress-activated protein kinase (JNK/SAPK) and p38, is a critical signaling in cells, which plays a notable role in

embryo development [5]. MAPK signaling has been found to mediate multiple biological behaviors of cells, including cell proliferation, differentiation, growth and apoptosis [5]. In addition, MAPK is reported to be involved in the growth and development of tooth germ [6-8]. In odontoblast-like cells, fluoride was found to activate MAPK activity, and the activating MAPK was then involved in the apoptosis of odontoblast-like cells [9]. However, the role and activity of MAPK remain unknown in ameloblasts till now.

The most toxic effect of fluoride is induction of apoptosis [10, 11], and fluoride has been proved to transmit from mother to child [12]. However, the effect of fluoride on ameloblasts has not been fully demonstrated in rat offspring. The aim of this study was to evaluate

Fluoride on ameloblasts and MAPKs and caspase-12 activity

the effect of fluoride on the ameloblasts in the offspring rat tooth germ, and explore the underlying mechanisms.

Materials and methods

Animals

Eighteen Sprague-Dawley rats with a female/male ratio of 1:1, each weighing 200-250 g, were purchased from the Laboratory Animal Center of Xi'an Jiaotong University (Xi'an, China). Rats were assigned to three groups (pairs of male and female). Animals in Group A (control) were given deionized water without sodium fluoride, and rats in Group B were given 50 mg/L sodium fluoride for successive 6 weeks, while animals in Group C were administered with 100 mg/L sodium fluoride for successive 6 weeks. All rats were housed in polypropylene cages and exposed to 10-12 h of daylight.

Tissue preparation

After maternal rat delivery, the offspring rats were sacrificed using a cervical dislocation method 3 days after birth. The mandible was collected, fixed in 4% paraformaldehyde for 24 h, decalcified in 10% ethylenediaminetetraacetic acid (EDTA) 4°C for one week. Then, the samples were extensively washed with 70% ethanol, dehydrated with a gradient series of ethanol (85%, 95% and 100%), made transparent in xylene, embedded in paraffin wax, and cut into 5 µm sections. Subsequent, the sections were stained with haematoxylin & eosin (HE), and mounted on polylysine-coated slides for immunohistochemical and TUNEL analyses. The remaining mandibles were immersed in liquid nitrogen for 1 h and then frozen at -80°C for subsequent experiments.

Immunohistochemistry

Sections were deparaffinized, rehydrated, and treated with 3% hydrogen peroxide for 20 min to block the endogenous peroxidase activity. Then, the sections were rinsed three times with PBS, and incubated with 5% (w/v) bovine serum albumin (BSA; Sigma; St. Louis, MO, USA) in PBS at room temperature for 20 min to block the non-specific binding. Subsequently, the slides were incubated in rabbit anti-ERK, anti-p-ERK, anti-p38, anti-p-p38 (Thr180/Tyr182), anti-JNK, and anti-p-SAPK/JNK (Thr183/Tyr-

185) polyclonal antibodies (1:200 dilution; Cell Signaling; Beverly, MA, USA), while those incubated in normal rabbit serum served as negative controls. Subsequently, sections were incubated in peroxidase-conjugated anti-mouse secondary antibody (Beijing Zhongshan Golden Bridge Biotechnology Co., Ltd.; Beijing, China) at 37°C for 30 min and washed 4 times with PBS, of 5 min each time. Immunoreactivity was visualized with 3-3-diaminobenzidine (DAB; Fuzhou Maixin Biotechnology Co., Ltd.; Fuzhou, China) substrate and counterstained with hematoxylin. The sections were then observed under a Leica DM750 optical microscope (Leica Microsystems; Wetzlar, Germany). The color intensity was calculated as an index of target protein expression. Finally, photo micrographs of the sections were taken using a Leica DM-2500 microscope (Leica Microsystems; Wetzlar, Germany).

TUNEL assay

TUNEL assay was performed using the kit provided by Nanjing KeyGen Biotech Co., Ltd. (Nanjing, China) following the manufacturer's instructions. Briefly, the embedded tissues were deparaffinized, rehydrated through graded alcohol series, washed 3 times with PBS (of 5 min each time) and permeabilized in 0.1% TritonX-100 for 5 min at room temperature. Following washing 3 times in PBS, the sections were incubated in 3% H₂O₂ for 20 min, washed in PBS, and treated with proteinase K (20 µg/ml) for 15 min at 37°C. Subsequently, each specimen was incubated in 100 µl of equilibrium buffer for 10 min, and then incubated in 50 µl of terminal deoxynucleotidyl transferase (TdT) buffer covered with a plastic coverslip at 37°C for 1 h, while sections that were run in PBS without TdT served as negative controls. Then, the sections were washed three times in PBS and incubated in stop/wash buffer at room temperature for 5 min. HRP-conjugated streptavidin was applied to sections at 37°C for 30 min, and then, sections were washed 3 times in PBS and developed with peroxidase substrate diaminobenzidine (DAB) for 5 min. Finally, ameloblasts were analyzed by microscopy.

Transmission electron microscopy

The mandibular molar tooth germ was collected from rats, fixed in 2.5% glutaraldehyde at

Fluoride on ameloblasts and MAPKs and caspase-12 activity

4°C for 24 h, and decalcified with 10% EDTA for 1 week. Subsequently, the specimens were treated with 1% osmic acid for 2 h, dehydrated through a gradient series of ethanol, and embedded as the general method. The sections were stained with uranyl acetate and lead citrate, observed and representative images were captured on a JEM-ARM200F transmission electron microscope (Hitachi; Tokyo, Japan). Ultrastructural changes of ameloblasts were observed using transmission electron microscopy.

Western blotting assay

The mandibular molar tooth germ stored at -80°C was sheared on ice using eye scissors. Tooth germ tissues were homogenized in a pre-cooled RIPA buffer (50 mM Tris-HCl pH 7.5, 50 mM NaCl, 5 mM EDTA, 10 mM EGTA, 2 mM sodium pyrophosphate, 4 mM paranitrophenylphosphate, 1 mM sodium orthovanadate, 1 mM phenylmethylsulfonyl fluoride, 2 mg/ml aprotinin, 2 mg/ml leupeptin and 2 mg/ml pepstatin). The homogenates were incubated on ice for 30 min and centrifuged at 12,000× g for 15 min at 4°C. The protein content was determined using a BCA protein assay kit (Pierce; Rockford, IL, USA). A volume corresponding to an equal protein mass for each supernatant was mixed with the loading buffer (5-sodium dodecyl sulfate, 5% v/v) and denatured by heating the samples at 95°C for 5 min. Lysate protein was resolved to size by electrophoresis using 10% to 12% sodium dodecyl sulfate polyacrylamide gel electrophoresis (SDS-PAGE) and transferred to 0.22 µm polyvinylidene fluoride (PVDF) membrane (Millipore; Bedford, MA, USA) using a semi-dry blotting system (Bio-Rad; Hercules, CA, USA). Non-specific absorption by the membranes was blocked by incubation with 5% (w/v) skim milk in Tris-buffered saline (TBS; 500 mM NaCl, 20 mM Tris-HCl pH 7.5, with 0.05% (v/v) Tween-20) for 2 h. Blots were incubated at 4°C overnight with one of the following primary antibodies, rabbit anti-ERK (1:1000; Cell Signaling; Beverly, MA, USA), anti-p-ERK (1:1000; Cell Signaling; Beverly, MA, USA), anti-JNK (1:500; Cell Signaling; Beverly, MA, USA), anti-p-JNK (1:500; Cell Signaling; Beverly, MA, USA), anti-p38 (1:500; Cell Signaling; Beverly, MA, USA), anti-p-p38 (1:500; Cell Signaling; Beverly, MA, USA), anti-caspase-3 (1:1000; Cell Signaling; Beverly, MA, USA) and anti-caspase-12 (1:1000; Bio-

Vision, Milpitas, CA, USA), each diluted in TBS with 5% (v/v) bovine serum containing 0.1% Tween-20 for 24 h at room temperature with gentle shaking, while β-actin (1:1000; Santa Cruz Biotechnology; Santa Cruz, CA, USA) served as controls. The membranes were washed using 0.1% Tween-20 TBS 3 times, of 10 min each time and incubated with HRP-conjugated anti-rabbit or anti-mouse secondary antibody (1:10000; Beijing Zhongshan Golden Bridge Biotechnology Co., Ltd.; Beijing, China) as appropriate for each primary antibody for 1 h at room temperature. After washing in TBS-0.1% Tween-20 three times, an enhanced chemiluminescence kit (Millipore; Bedford, MA, USA) was used to detect immunoreactive protein bands. Blots were immune-detected with an anti-β-actin antibody to confirm equal mass of protein loaded among samples. The intensity for each immunoreactive protein band was quantified using a Quantity One densitometer (BioRad; Hercules, CA, USA).

Ethical statement

This study was approved by the Ethical Review Committee of Hospital of Stomatology, Xi'an Jiaotong University (permission No. 201300-12). All animal experiments were performed in compliance with the National Guidelines for the Breeding, Care, and Management of Laboratory Animals in China ([2011]588).

Statistical analysis

All experimental data were expressed as mean ± standard deviation (SD), and all statistical analyses were performed using the statistical software SPSS version 11.5 (SPSS, Inc.; Chicago, IL, USA). Differences of means were tested for statistical significance with one-way analysis of variance (ANOVA), followed by Tukey's multiple comparison test. A *P* value of < 0.05 was considered statistically significant.

Results

Appearance of rat incisors

The control rats had yellow, glossy and high-transparency incisor labial surface (**Figure 1A**), while the rats given 50 mg/L fluoride-containing water had yellow-brown thin streaks on the incisor labial surface, which were more notable in mandibular incisors (**Figure 1B**). However, the rats given 100 mg/L fluoride-contain-

Fluoride on ameloblasts and MAPKs and caspase-12 activity

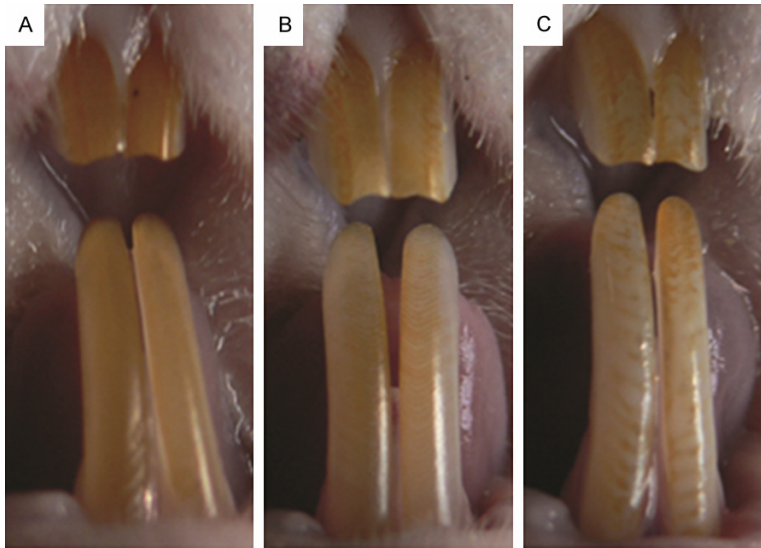


Figure 1. Changes in appearance of rat incisors following fluoride treatment. A: Controls; B: Low-fluoride group (50 mg/L sodium fluoride); and C: High-fluoride group (100 mg/L sodium fluoride).

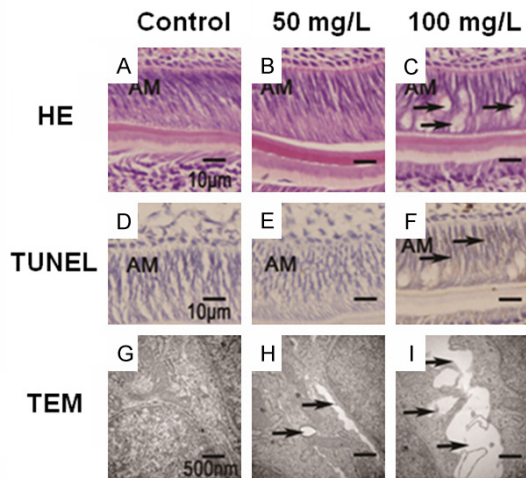


Figure 2. Morphological changes of tooth germ ameloblasts in offspring rats. A-C: HE staining, scale bar = 10 μ m; D-F: TUNEL assay, scale bar = 10 μ m; and G-I: TEM, scale bar = 500 nm.

ing water had clear yellow-brown or white streaks on the incisor labial surface and the regions close to the cutting edge of the incisor, which were more notable in mandibular incisors (**Figure 1C**).

Morphology of tooth germ ameloblasts in offspring rats

HE staining showed tidily arranged ameloblasts on the mandibular molar tooth germ of the

control rat offspring, and enamel matrix was secreted on the dentin surface; in addition, odontoblast process was observed, indicating the penetration of the Tomes' process into the enamel matrix, and the enamel matrix was found to be evenly stained in red (**Figure 2A**). Similar morphology of ameloblasts was seen in the offspring of the rats given 50 mg/L fluoride-containing water as compared to the controls (**Figure 2B**), while in the 100 mg/L fluoride-containing water-fed rat offspring, degeneration and vacuolar changes of ameloblasts were seen, with intracellular space found among ameloblasts, and a large number of vacuoles were observed in the basal part of the ameloblasts (**Figure 2C**).

number of vacuoles were observed in the basal part of the ameloblasts (**Figure 2C**).

TEM revealed oval ameloblast nucleus on the tooth germ of the control rat offspring, with obvious nucleolus and abundant organelles seen, and abundant rough endoplasmic reticulum and ribosome, and ameloblastic matrix vesicles were found in the cytoplasm (**Figure 2G**). In the offspring of the rats given 50 mg/L fluoride-containing water, vacuoles of unequal sizes were found to be scattered among the ameloblasts on the tooth germ, with enlargement of rough endoplasmic reticulum and intracellular space among ameloblasts, and perinuclear space was found (**Figure 2H**). In the offspring of the rats given 100 mg/L fluoride-containing water, a large number of vacuoles were observed among the ameloblasts on the tooth germ, and remarkable enlargement of rough endoplasmic reticulum, intracellular space disappearance and replacement by vacuoles, and mitochondria swelling and deformation were found in ameloblasts (**Figure 2I**).

Apoptosis of tooth germ ameloblasts in offspring rats

TUNEL assay showed no yellow-brown granules in the tooth germ ameloblast nucleus of the offspring of the control rats (**Figure 2D**) or rats given 50 mg/L fluoride-containing water (**Figure 2E**), while yellow-brown granules were found in

Fluoride on ameloblasts and MAPKs and caspase-12 activity

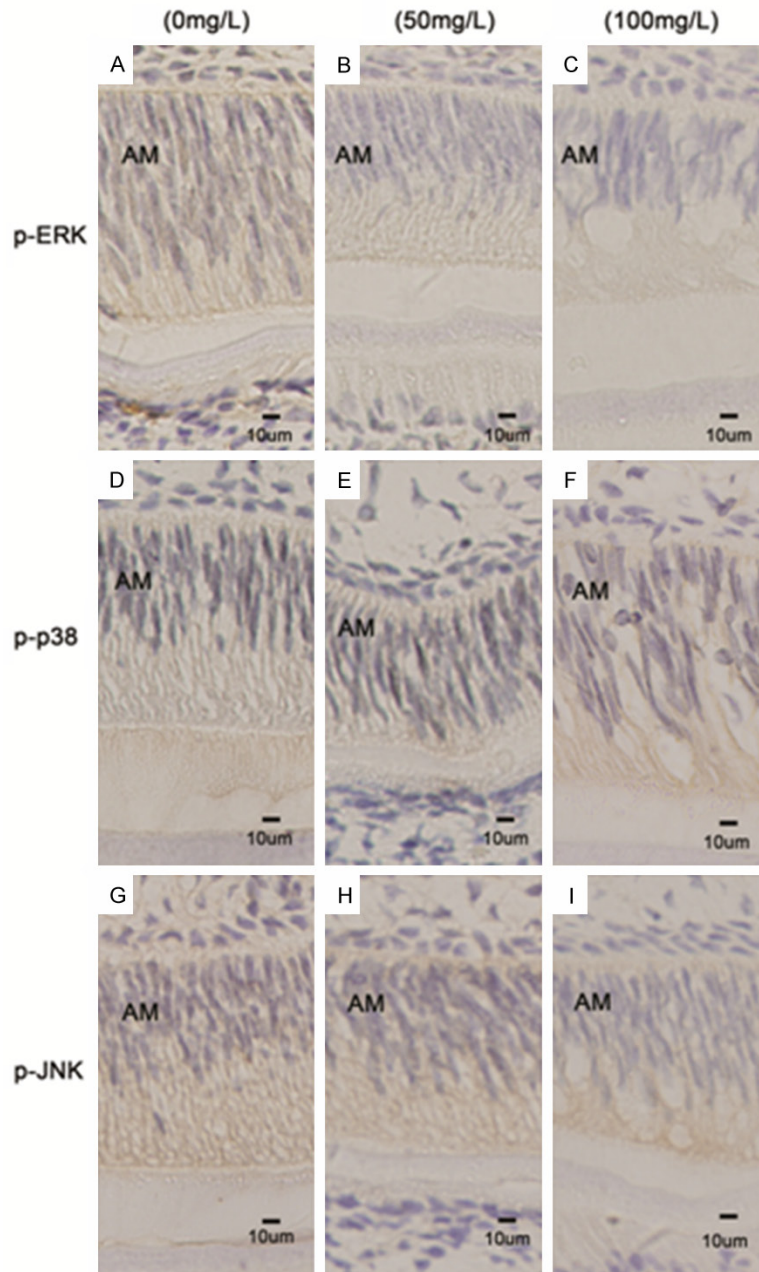


Figure 3. Immunohistochemical staining of MAPKs in tooth germ ameloblasts in offspring rats. A-C: p-ERK expression; D-F: p-p38 expression; G-I: p-JNK expression; A, D, G: Controls; B, E, H: 50 mg/L sodium fluoride; and C, F, I: 100 mg/L sodium fluoride. Scale bar = 10 µm.

the ameloblast nucleus derived from the high-fluoride group (**Figure 2F**).

Expression of MAPK signaling protein in the tooth germ ameloblasts of the offspring rats

Immunohistochemistry detected ERK (p-ERK), p38 (p-P38) and JNK (p-JNK) phosphorylation in the tooth germ ameloblasts of all offspring

rats at various levels (**Figure 3**), and the p-ERK and p-JNK expression was found to reduce while the p-P38 expression increased with the rise in the fluoride concentration in the water given to the parental rats ($P < 0.05$).

Western blotting analysis showed reduced p-ERK and p-JNK and increased p-p38 expression in the tooth germ ameloblasts of the offspring rats with the rise in the fluoride concentration in the water given to the parental rats (**Figure 4**). In addition, fluoride was found to dose-dependently reduce the p-ERK and p-JNK expression and increase the p-p38 expression ($P < 0.05$).

Expression of caspase-3, caspase-8, caspase-9 and caspase-12 in the tooth germ ameloblasts of the offspring rats

Western blotting assay revealed reduced caspase-3 expression in the tooth germ ameloblasts of the offspring rats with the rise in the fluoride concentration in the water given to the parental rats ($F = 59.83$, $P < 0.01$), and there was a significant difference in the caspase-3 expression between the high- and low-fluoride groups ($P < 0.01$), while no significant difference was seen between the low-fluoride and control groups ($P > 0.05$) (**Figure 5A**). The

caspase-12 expression was found to reduce with the rise in the fluoride concentration in the water given to the parental rats ($F = 10.58$, $P < 0.05$), and higher caspase-12 expression was detected in the controls than in the low- ($P < 0.05$) and high-fluoride groups ($P < 0.01$) (**Figure 5B**). In addition, reduced caspase-8 ($F = 33.75$, $P < 0.01$) and caspase-9 expression ($F = 44.06$, $P < 0.05$) was observed with the

Fluoride on ameloblasts and MAPKs and caspase-12 activity

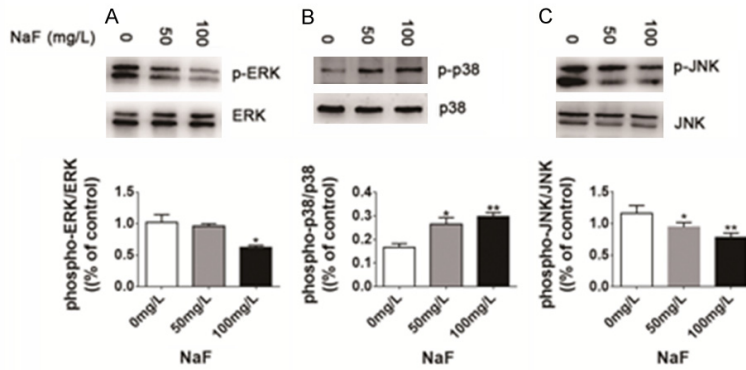


Figure 4. Western blotting determines MAPKs expression in tooth germ ameloblasts in offspring rats. A: ERK and p-ERK expression; B: p38 and p-p38 expression; and C: JNK and p-JNK expression.

rise in the fluoride concentration in the water given to the parental rats, and significant differences were seen in the caspase-8 and caspase-9 expression between the high-fluoride and control groups ($P < 0.05$), while no significant difference was detected in caspase-8 or caspase-9 expression between the low-fluoride and control groups ($P > 0.05$) (Figure 5C and 5D).

Discussion

Our findings showed morphological changes in the incisor of rats following treatment with fluoride-containing water for 6 weeks, which were characterized by yellow-brown thin streaks on the incisor labial surface, with more notable changes seen in mandibular incisors. These findings suggest the successful modeling of dental fluorosis in rats [13-15]. In the current study, female and male rats in groups B and C were given sodium fluoride since caged, and the female rats were still administered with fluoride-containing water during pregnancy, while the control rats were given deionized water without sodium fluoride. The results demonstrate that fluoride may enter the rat offspring via the placenta and affect the tooth germ of the offspring rats, resulting in morphological changes on the tooth germ ameloblasts of the offspring rats. Under an optical microscope, vacuole-like changes were seen in the cytoplasm of ameloblasts, notably in the offspring of rats given 100 mg/L fluoride-containing water. TEM displayed enlargement of endoplasmic reticulum and intracellular space among ameloblasts on the tooth germ in the offspring

of the rats given 50 mg/L fluoride-containing water; however, this enlargement was not remarkable, resulting in no ultrastructural changes of ameloblasts seen under the optical microscope. In the offspring of the rats given 100 mg/L fluoride-containing water, obvious ultrastructural changes were observed on the ameloblasts of the tooth germ, with significant enlargement of endoplasmic reticulum, clear-cut increase in intracellular space and mitochondrial swelling seen in

ameloblasts, resulting in a large number of vacuoles observed in the cytoplasm of ameloblasts under an optical microscope. These vacuoles are considered as the organelles of mitochondrial swelling.

The fluoride cytotoxicity is accepted as fluoride-induced apoptosis [13-16]. In the present study, *in situ* TUNEL assay was performed to detect the apoptosis of ameloblasts on the tooth germ of fluoride-treated rat offspring. Our findings showed no yellow-brown granules in the tooth germ ameloblast cytoplasm of the offspring of the control rats or rats given 50 mg/L fluoride-containing water, while yellow-brown granules were widely found in the cytoplasm of ameloblasts with vacuole-shaped degeneration derived from the high-fluoride group. The data suggest that fluoride may enter the offspring rats through the parental rat placenta and dose-dependently affect the morphology and ultrastructure of ameloblasts on the offspring rat tooth germ; in addition, high-concentration fluoride causes apoptosis of ameloblasts in the tooth germ of the offspring rats.

It has been found that fluoride increases MAPK expression in odontoblasts, and the activation of MAPK is involved in the apoptosis of odontoblasts [9]. On the contrast, MAPK activity was also reported to play a critical role in the growth and development of tooth germ, and was involved in the entire development process of tooth germ [6-8]. However, the activity of MAPK remains unknown in ameloblasts. In this study, we measured MAPK activity in the ameloblast on the offspring rat tooth germ, and the p-ERK

Fluoride on ameloblasts and MAPKs and caspase-12 activity

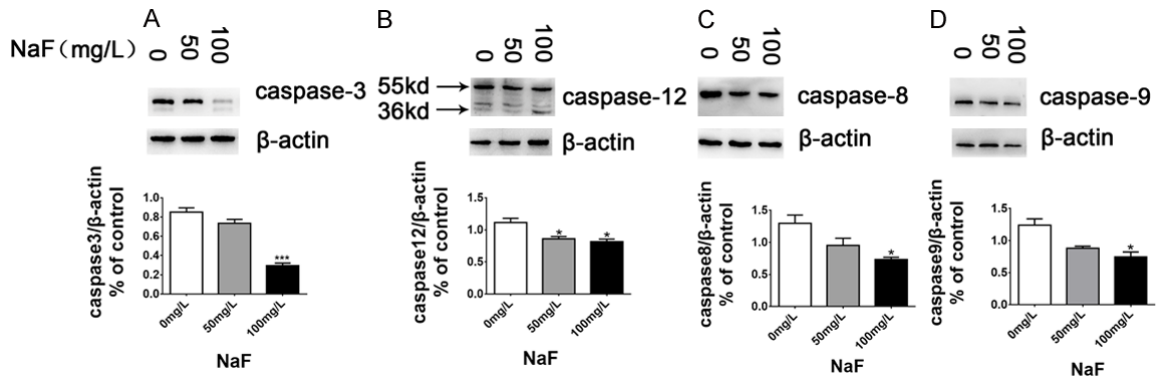


Figure 5. Western blotting determines caspase-3, caspase-8, caspase-9 and caspase-12 expression in tooth germ ameloblasts in offspring rats. A: Caspase-3 expression; B: Caspase-12 expression; C: Caspase-8 expression; and D: Caspase-9 expression.

and p-JNK expression decreased and the p-p38 expression increased with the fluoride concentration, which was in agreement with previous reports [6-8]. NaF treatment was found to down-regulate p-JNK expression, which was involved in the down-regulation of MMP-20 synthesis [17]. As a member of MAPK family, p38 has been proved to participate in apoptosis [18, 19]. In the present study, we detected apoptosis in a large number of ameloblasts on the tooth germ of offspring rats. Taking these findings together, it is considered that MAPK is involved in the development of dental fluorosis. Further *in vitro* experiments were required to examine the correlation between up-regulation of p38 expression and ameloblast apoptosis following fluoride treatment.

Caspase has been identified as a key enzyme involved in cell apoptosis [20]. Caspase-8 and caspase-9, which act as initiators, are key enzymes that trigger mitochondrial and death receptor pathways, and activation of caspase-3, a master switch of apoptosis and caspase effector, results in entrance in cell apoptosis, which is indicative of the initiation of apoptosis [21-23]. Caspase-12, a cysteine protease localized in the endoplasmic reticulum, was reported to activate directly caspase-3, and allow the process into apoptosis [24-26]. Since NaF was found to affect endogenous and exogenous apoptotic pathways, fluoride-induced apoptosis is considered to be mediated by mitochondrial and death receptor pathways [13]. In this study, remarkable enlargement of rough endoplasmic reticulum was in ameloblasts in the high-fluoride group, and activation of caspase-3, cas-

pase-8, caspase-9 and caspase-12 was detected on the tooth germ of the offspring rats. Our data suggest that endoplasmic reticulum-mediated caspase-12 activation is involved in fluoride-induced ameloblast apoptosis, in addition to mitochondrial and death receptor pathways, and fluoride mediates ameloblast apoptosis in a dose-dependent manner.

In summary, the results of the present study demonstrate that high-concentration fluoride treatment causes morphological and ultrastructural changes and apoptosis in the tooth germ ameloblasts of the rat offsprings. MAPK signaling is involved in dental fluorosis, and the p-ERK and p-JNK expression is down-regulated while p-p38 expression is up-regulated dose-dependently with the fluoride concentration. In addition, caspase-12 may be involved in fluoride-induced ameloblast apoptosis.

Acknowledgements

This study was supported by the National Natural Science Foundation of China (grant No. 30972558).

Disclosure of conflict of interest

None.

Address correspondence to: Jian-Ping Ruan, Clinical Research Center of Shaanxi Province for Dental and Maxillofacial Diseases, Department of Preventive Dentistry, Stomatology Hospital, Xi'an Jiaotong University, 98 Xiwu Road, Xi'an 710004, Shaanxi Province, China. Tel: 029-87275706; Fax: 029-87275706; E-mail: ruanjp@mail.xjtu.edu.cn

Fluoride on ameloblasts and MAPKs and caspase-12 activity

References

- [1] Denbesten P, Li W. Chronic fluoride toxicity: dental fluorosis. *Monogr Oral Sci* 2011; 22: 81-96.
- [2] Aoba T, Fejerskov O. Dental fluorosis: chemistry and biology. *Crit Rev Oral Biol Med* 2002; 13: 155-170.
- [3] Khan A, Moola MH, Cleaton-Jones P. Global trends in dental fluorosis from 1980 to 2000: a systematic review. *SADJ* 2005; 60: 418-421.
- [4] Hu DY, Hong X, Li X. Oral health in China-trends and challenges. *Int J Oral Sci* 2011; 3: 7-12.
- [5] Seger R, Krebs EG. The MAPK signaling cascade. *FASEB J* 1995; 9: 726-735.
- [6] Cho KW, Cai J, Kim HY, Hosoya A, Ohshima H, Choi KY, Jung HS. ERK activation is involved in tooth development via FGF10 signaling. *J Exp Zool B Mol Dev Evol* 2009; 312: 901-911.
- [7] Lee MJ, Cai J, Kwak SW, Cho SW, Harada H, Jung HS. MAPK mediates Hsp25 signaling in incisor development. *Histochem Cell Biol* 2009; 131: 593-603.
- [8] Cho KW, Cho SW, Lee JM, Lee MJ, Gang HS, Jung HS. Expression of phosphorylated forms of ERK, MEK, PTEN and PI3K in mouse oral development. *Gene Expr Patterns* 2008; 8: 284-290.
- [9] Karube H, Nishitai G, Inageda K, Kurosu H, Matsuoka M. NaF activates MAPKs and induces apoptosis in odontoblast-like cells. *J Dent Res* 2009; 88: 461-465.
- [10] Chen J, Cao J, Wang J, Jia R, Xue W, Xie L. Fluoride-induced apoptosis and expressions of caspase proteins in the kidney of carp (*Cyprinus carpio*). *Environ Toxicol* 2015; 30: 769-781.
- [11] Agalakova NI, Gusev GP. Molecular mechanisms of cytotoxicity and apoptosis induced by inorganic fluoride. *ISRN Cell Biol* 2012; 2012: 403835.
- [12] Driscoll WS. A review of clinical research on the use of prenatal fluoride administration for prevention of dental caries. *ASDC J Dent Child* 1981; 48: 109-117.
- [13] Barbier O, Arreola-Mendoza L, Del Razo LM. Molecular mechanisms of fluoride toxicity. *Chem Biol Interact* 2010; 188: 319-333.
- [14] Bogatcheva NV, Wang P, Birukova AA, Verin AD, Garcia JG. Mechanism of fluoride-induced MAP kinase activation in pulmonary artery endothelial cells. *Am J Physiol Lung Cell Mol Physiol* 2006; 290: L1139-L1145.
- [15] Yang T, Zhang Y, Li Y, Hao Y, Zhou M, Dong N, Duan X. High amounts of fluoride induce apoptosis/cell death in matured ameloblast-like LS8 cells by downregulating Bcl-2. *Arch Oral Biol* 2013; 58: 1165-1173.
- [16] Zhang M, Wang A, He W, He P, Xu B, Xia T, Chen X, Yang K. Effects of fluoride on the expression of NCAM, oxidative stress, and apoptosis in primary cultured hippocampal neurons. *Toxicology* 2007; 236: 208-216.
- [17] Zhang Y, Yan Q, Li W, DenBesten PK. Fluoride down-regulates the expression of matrix metalloproteinase-20 in human fetal tooth ameloblast-lineage cells in vitro. *Eur J Oral Sci* 2006; 114: 105-110.
- [18] Ishikawa Y, Kitamura M. Dual potential of extracellular signal-regulated kinase for the control of cell survival. *Biochem Biophys Res Commun* 1999; 264: 696-701.
- [19] Eom HJ, Choi J. p38 MAPK activation, DNA damage, cell cycle arrest and apoptosis as mechanisms of toxicity of silver nanoparticles in Jurkat T cells. *Environ Sci Technol* 2010; 44: 8337-8342.
- [20] Salvesen GS. Caspases and apoptosis. *Essays Biochem* 2002; 38: 9-19.
- [21] Matalova E, Svandova E, Tucker AS. Apoptotic signaling in mouse odontogenesis. *OMICS* 2012; 16: 60-70.
- [22] Shi Y. Mechanisms of caspase activation and inhibition during apoptosis. *Mol Cell* 2002; 9: 459-470.
- [23] Zheng TS, Hunot S, Kuida K, Flavell RA. Caspase knockouts: matters of life and death. *Cell Death Differ* 1999; 6: 1043-1053.
- [24] Nakagawa T, Zhu H, Morishima N, Li E, Xu J, Yankner BA, Yuan J. Caspase-12 mediates endoplasmic-reticulum-specific apoptosis and cytotoxicity by amyloid-beta. *Nature* 2000; 403: 98-103.
- [25] Szegezdi E, Fitzgerald U, Samali A. Caspase-12 and ER-stress-mediated apoptosis: the story so far. *Ann N Y Acad Sci* 2003; 1010: 186-194.
- [26] Hitomi J, Katayama T, Taniguchi M, Honda A, Imaizumi K, Tohyama M. Apoptosis induced by endoplasmic reticulum stress depends on activation of caspase-3 via caspase-12. *Neurosci Lett* 2004; 357: 127-130.